ELSEVIER

Exchange Rates of Ethanol with Water in Water-Saturated Cement Pastes Probed by NMR

Hans C. Gran* and Eddy W. Hansen†
*Norwegian Building Research Institute and Department of Chemistry, University of Oslo, and
†SINTEF Oslo, Oslo, Norway

Diffusion of ethanol into water-saturated white cement pastes has been investigated by carbon and proton nuclear magnetic resonance (NMR). The diffusion of ethanol was shown to be Fickian, assuming one-dimensional diffusion under perfect sink boundary conditions. Derived diffusion coefficients were found to increase with increasing water/cement (w/c) ratio from (2.7 ± 0.5) 10^{-8} cm^2/s at w/c = 0.30 to (59 ± 5) 10^{-8} cm^2/s at w/c = 1.0. At the end of the exchange process, only a fraction of the total volume of water is exchanged with ethanol, varying from 60% for samples containing mainly micro- and mesopores to about 80% for samples where additional capillary pores are present. Time needed to reach 90% and 95% exchange of the total intrudable amount of ethanol in cylindrical samples with diameter of 5.5 mm varied from 1 day to nearly 3 weeks. This has importance for exchange in larger samples with typical diameters of 10 mm or more (as used in mercury intrusion porosimetry), which may require on the order of months for 90% exchange to take place. The mole fraction of ethanol and water in the pore system was determined from sampled carbon and proton NMR spectra vs. exchange time by comparing H_2O-saturated and D_2O-saturated samples. At the end of the exchange process, water was found to occupy the remaining volume not accessible to ethanol. In the tested w/c ratio range, the water content in all samples is below the value where damage to the pore structure normally occurs due to internal tension when exposed to drying. An empirical relationship between chemical shift of the CH_3CH_2OH/H_2O peak and mole fraction of ethanol is derived, enabling the mole fraction of ethanol from the NMR peak to be estimated. ADVANCED CEMENT BASED MATERIALS 1998, 8, 108–117. © *1998 Elsevier Science Ltd.*

KEY WORDS: Nuclear magnetic resonance, Liquid exchange, Diffusion, Cement paste

The exchange or liquid replacement of water by ethanol in the porous structure of hydrated cement paste (HCP) and concrete is used where gentle drying is required to preserve the porous structure and to reduce the danger of introducing microcracks. Applications are, among others, found in mercury intrusion porosimetry (MIP) [1] and optical microscopy [2]. The sample is normally placed in a reservoir of ethanol or another alcohol for several days. After replacement, the ethanol is removed by evaporation. One recent application is in optical ultraviolet microscopy of concrete, where a combination of gentle drying and impregnation of the concrete with a solution of ethanol and a fluorescent dye (fluorescent liquid replacement [FLR] technique) [3] is done to observe air voids, cracks, variations in density, and the water-to-cement mix ratio (w/c ratio) in very dense samples. The FLR technique is a quantitative application where the intensity of fluorescent light from the samples is used to determine the w/c ratio [3,4]. Determination of the w/c ratio is dependent on the amount of exchange of ethanol for water. To be accurate and reliable, the technique will require that a sufficient and known degree of exchange be achieved. It is also important to know the time needed for sufficient exchange to take place. ^1H nuclear magnetic resonance (NMR) carried out on ethanol surrounding samples (diameter 3.5 mm) of hydrated cement pastes with a w/c ratio of 0.40 has shown that about 60% to 70% of the pore water is exchanged during a period of a few days [3]. Most recently, the diffusion of ethanol into water saturated HCPs (also w/c = 0.40) has been monitored by observing the ^{13}C-NMR signal intensity of ethanol vs. time during exchange with water [5]. A large difference in exchange rates between preheated and virgin samples was observed. Both works demonstrate the capability of NMR as a quantitative and nondestructive experimental technique in characterization of HCP.

However, knowledge of the effect of w/c ratio on both exchange rate and amount of exchange is still needed. Furthermore, the amount of water present in the pore structure after an exchange process has taken place is important. Water, through its surface tension, may set up destructive forces within the pore structure

Address correspondence to: Dr. Hans C. Gran, Norges byggforskningsinstitutt, Postboks 123 Blindern, 0314, Oslo, Norway.
Received December 6, 1996; Accepted January 14, 1998

ISSN 1065-7355/98/$19.00
PII S1065-7355(98)00013-3

during the final drying that normally succeeds liquid exchange. HCPs are particularly vulnerable at relative humidities between about 45% and 90% [6]. A relative humidity of 45% corresponds to water contents occupying between 85% and 40% of the total pore space in the w/c ratio range 0.30 to 1.0 [7]. As liquid exchange is normally succeeded by drying to remove the alcohol, it is therefore important for an exchange process to reach water contents below these values.

In light of this, we have first monitored the exchange of ethanol for pore water in HCPs vs. w/c ratios by observing the intensity (integrated area) of the ^{13}C-NMR peaks from the ethanol entering the pore system as a function of time. From this, diffusion coefficients have been calculated. Second, as ^{13}C-NMR alone does not give information about the amount of water still present in the pore structure, in a separate series of experiments we monitored both ^{1}H-NMR and ^{13}C-NMR intensities. In order to calculate the mole fraction ethanol/water in the pore system, both ^{1}H-NMR and ^{13}C-NMR have been applied on a D_2O-saturated HCP where the contribution from water protons is not present. The amount of water and ethanol derived from these NMR measurements is compared to the total amount determined gravimetrically.

Finally, a nonlinear least squares curve fitting analysis, or deconvolution of the ^{1}H-NMR spectrum, is applied in order to derive a possible correlation between chemical shift and mole fraction. Typical high resolution (HR) ^{1}H-NMR spectra from a mixture of ethanol and water contain three separate peaks. The three peaks correspond to the methyl and methylene groups of ethanol and—when fast exchange condition is satisfied—one peak originating from the ethanol OH group and water. The amount of hydrogen bonding and thus the electronic surroundings of a proton depend critically on the relative concentrations of ethanol and water. The chemical shift of the OH/H_2O proton peak is expected to depend on the relative concentration of ethanol and water.

Experimental

Sample Preparation

Four different samples of HCPs with w/c ratios of 0.30, 0.40, 0.60, and 1.0 were prepared for ^{13}C-NMR measurements of the amount of exchange and diffusion of ethanol. The samples, which were prepared with distilled water, were between 2 and 3 years old at the time of analysis and are referred to as S03, S04, S06, and S10, respectively. Two samples, S1 and S2, were prepared for ^{1}H-NMR measurements. These were made from two 3-month-old HCPs with w/c ratio of 0.40. Sample S2 differed from S1 in being hydrated using D_2O instead of H_2O. To reduce influence of paramagnetic constituents, all pastes were made from a Danish Super White Portland Cement certified as a British Standards Institution class 62.5N cement, with a Bogue composition of 65.8% tricalcium silicate (C_3S), 21.0% dicalcium silicate (C_2S), 4.18% tricalcium aluminate (C_3A), and 0.96% tetracalcium alumina ferrite (C_4AF), and a Blaine surface of 4000 cm^2/g. The content of paramagnetic constituents Fe_2O_3 and Mn_2O_3 were 0.31% and 0.012% by weight of cement, respectively. All pastes were mixed under vacuum, and molded and sealed in cylindrical polytetrafluoroethane forms with diameter of 20 mm and length of 120 mm. The pastes were slowly rotated during the first 20 hours of hardening to avoid separation between water and cement. After demolding, the H_2O pastes were stored in water at room temperature until testing. The D_2O paste was similarly stored in D_2O. Samples S03, S04, S06, S10, and S1 were tested in virgin condition, i.e., without any pretreatment. Sample S2 was preheated at 105°C for a period of 12 hours and resaturated with D_2O prior to the test.

To fit into the NMR tubes and the radiofrequency receiver/transmitter coil, the samples were cut to cylindrical shape with a diameter of 5.5 mm and a length of 20 mm (samples S03, S04, S06, and S10) and 3.5 mm, and a length of 10 mm (samples S1 and S2). To obtain quantitative measurements the whole length of the sample was placed within the receiver/transmitter coil. The NMR tubes were closed with an airtight cap and weighed before and after acquisition.

Four samples (R03, R04, R06, and R10) of HCPs corresponding to w/c ratios 0.30, 0.40, 0.60 and 1.0 were saturated with ethanol and served as references for determination of the actual amount of ethanol in samples S03, S04, S06, and S10 during the tests. These reference samples were first stored for 2 weeks in ethanol to avoid development of microcracks, preheated at 105°C until the weight remained constant, and then resaturated with reagent grade anhydrous ethanol. The resaturation was done by first storing the reference samples in ethanol vapor for 3 days and then immersing them in ethanol until constant weight was reached. The reference samples differed from the rest of the samples in consisting of two thin slices. Each slice cut to a rectangular shape 5 mm × 20 mm and with a thickness of 1 mm. This was done to ensure sufficient filling of the pore structure as, in particular, the samples with the lower w/c ratios showed considerably reduced resaturation rates. Initial weight, weight loss at 105°C, weight of ethanol, and degree of resaturation with ethanol (assuming bulk densities of the pore liquids, see later in the text) is shown in Table 1. To check the reproducibility of the resaturation process, a set of eight samples were additionally taken at w/c ratio 0.30, preheated at 105°C, and tested gravimetri-

Advn Cem Bas Mat
1998;8:108–117

TABLE 1. Weight of reference samples in saturated surface dry condition, m_{SSD}, weight loss at 105°C, m_{loss}, and weight of ethanol that has entered the reference sample, m_{et}

w/c	m_{SSD}	m_{loss}	$\frac{m_{loss}}{(\%)}$	m_{et}	F_{max}
0.30	1.206	0.163	13.5	0.0715	56.2
0.40	1.056	0.194	18.4	0.106	69.5
0.60	1.032	0.286	27.7	0.196	87.7
1.0	0.797	0.343	43.0	0.254	94.2

Note: Maximum degree of resaturation (F_{max}) with ethanol in percent is calculated (assuming bulk densities of the pore liquids) by correcting for ethanol density (i.e., volume of evaporated water equals m_{loss} and $V_{et} = m_{et}/(\delta_{et} m_{loss})$.

cally for loss of evaporable water. Standard deviation was calculated to be <1.0%.

A drying temperature of 105°C was selected, as this is a commonly used conventional procedure for determination of the amount of evaporable water in a sample of HCP. The difference in weight before and after drying is defined as the weight of evaporable water.

NMR Measurements

The experiments were performed on two different NMR spectrometers. Samples S03, S04, S06, and S10 were tested on a Bruker Avance DMX 200 NMR spectrometer, operating at 200-MHz proton resonance frequency using a 10-mm ^{13}C-NMR broadband probehead without proton decoupling. The bandwidth was set to 100 kHz using an acquisition time of 0.041 s. The applied 90° pulse length was 8.0 μs. The dead time was 7.14 μs. The total number of transients (radiofrequency [RF] pulses) was first set to 1024 for samples S04, S06, and S10 and 3072 for sample S03 to compensate for the lower content of ethanol. (Probably due to the application of prolonged high power pulsing and the fact that the reference samples were sliced, reference sample R03 showed a tendency to lose weight during the early experiments. The number of transients for this particular sample was in the end reduced to 1024, resulting in an inevitable reduction in signal-to-noise ratio.) The spin-lattice relaxation time, T_1, was measured in each sample using a simple inversion recovery (180°–τ–90°) pulse sequence. The longer T_1 of 189 ms was measured in sample S10, which contained the larger pore volume. The repetition time between RF pulses was set to 1 s, which is more than five times the spin-lattice relaxation time, and assures quantitative sampling of the spectrum.

Samples S1 and S2 were tested on a Varian VXR 300S NMR spectrometer, operating at 300-MHz proton resonance frequency using an HR 5-mm probehead. Both ^{1}H and ^{13}C-NMR experiments were carried out. The ^{13}C experiments were performed using a bandwidth of 20 kHz, with an acquisition time of 0.30 s and an RF pulse length of 8.2 μs. The number of accumulations was set to 1024. The ^{1}H-NMR experiments were performed using a bandwidth of 25 kHz, with an acquisition time of 1.3 s, an RF pulse length of 0.2 μs, and a dead time of 10 μs. Good signal-to-noise ratio was achieved with only four accumulations. The pulse repetition time was set to 1 s for both ^{1}H and ^{13}C-NMR acquisitions. The ^{13}C-NMR spectra were accumulated using gated decoupling, i.e., decoupling of the protons during acquisition time only, to exclude differential nuclear Overhauser effects (NOE) [8]. All NMR measurements were performed at room temperature of 25°C.

The experiments were carried out by immersing the samples of HCP in a reservoir of 10-ml 100% ethanol. The amount of ethanol entering the pore system of the sample as a function of time was measured by recording the proton and carbon NMR spectra at appropriate time intervals during the exchange process. Before each measurement, the samples were taken out of the ethanol, wiped dry with an absorbant tissue, weighed, and transferred to a 5-mm NMR tube. The samples were put back into the ethanol immediately after recording of the NMR spectra. During the initial stage of the process, the ethanol was changed between each experiment to avoid water concentration building up in the ethanol.

The ^{13}C-NMR spectra contained two peaks corresponding to the methylene and methyl carbons in the ethanol. The peaks were easily separated, having a line width of about 2.5 ppm and situated about 12 ppm apart. The amount of ethanol was proportional to the average peak intensity (integrated areas) of the two peaks and was normalized by setting the peak intensity of the reference sample with w/c ratio 1.0 to unity. The intensity of the reference sample was measured between every fifth experiment. Within experimental error, no drift was observed during the time of the experiments. In addition to the peaks from the ethanol, a broader peak from the ^{13}C broadband probehead could be observed. This broad peak was removed by subtraction using a spectrum that was accumulated with identical acquisition parameters on a ^{13}C-free hydrated cement sample.

The ^{1}H-NMR peaks were broadened to several hundred Hertz due to a combined effect of susceptibility differences (between the solid matrix and the pore liquid) and shortening of the spin-spin relaxation time due to restricted motional freedom resulting in severe overlapping between the OH, methyl, and methylene peaks. As a consequence, the proton spectra had to be deconvoluted by fitting them to a sum of three line shape functions by a nonlinear least squares technique. The choice of line shape functions were either Lorentzian or Gaussian or a combination of the two.

Water confined in a pore system is normally consid-

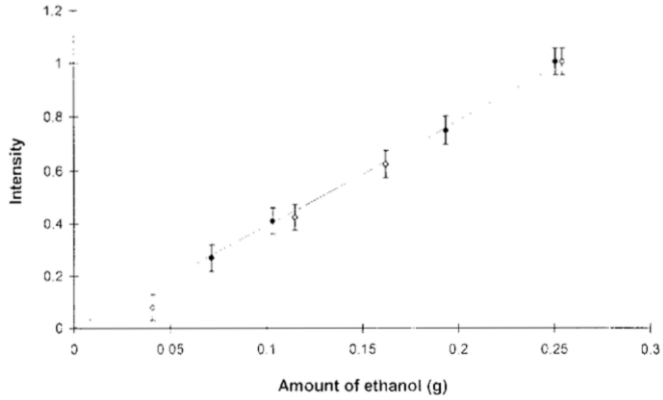

FIGURE 1. Measured ^{13}C-NMR peak areas of methylene and methyl peaks vs. amount of ethanol in the pore system of the reference samples. The dotted line represents a linear least squares fit to w/c ratios 0.30, 0.40, 0.60, and 1.0 in fully resaturated condition (●). Repeated experiments on the sample with w/c = 1.0 showed the uncertainty to be an absolute value of approximately 5%. At lower water contents (lower w/c ratios), the uncertainties are thus comparatively larger as indicated by the added error bars. ^{13}C-NMR peak areas observed in a partially filled hydrated cement paste represented by w/c = 1.0 exposed to stepwise drying is also presented (○).

ered to be separated into two different phases. One category corresponds to water situated in the bulk regions of the pore system, which is characterized by long spin-spin relaxation times. The second phase consists of water close to the pore surfaces and is characterized by a significantly shorter spin-spin relaxation time and is rather difficult, if not impossible, to detect without application of a spin-echo pulse sequence. However, since this work only deals with liquid-saturated pore systems, the interpretation of NMR data in this work may therefore be based on the existence of fast exchange between water near the pore surfaces and water in the bulk pore regions. Fast exchange on an NMR time scale causes an averaging of the spin-spin relaxation time. The existence of fast exchange in saturated hydrated cement pastes was shown by Bhattacharja et al. [9]. For this reason only a single RF pulse was applied for data acquisition.

Results and Discussion

References

Figure 1 shows the average peak area of the methylene and methyl ^{13}C-NMR resonance from ethanol, I_{et}, plotted vs. the gravimetrically determined amount of ethanol, m_{et}. The plot shows a linear relationship within the actual w/c ratio range investigated of samples fully saturated with ethanol. For partially saturated samples (containing different amounts of ethanol), the relation between NMR ^{13}C intensities and gravimetrically determined contents of ethanol shows a significant deviation from a straight line, suggesting that fast exchange condition is not satisfied. However, since in this work only saturated samples are investigated, Figure 1 shows that the fast exchange condition is satisfied.

A linear least squares fit to the data is shown as a dotted line in Figure 1. The slope was determined to 3.91 (±0.19) relative NMR peak area units/g (the relative ^{13}C-NMR peak area unit of reference sample with w/c = 1.0 chosen as unity).

Amount of Exchange

Calculation of the amount of ethanol, m_{et}, that has entered the pore system at any time during the exchange process is based on the empirical linear correlation in Figure 1 between m_{et} and the intensity, I_{et}, (eq 1):

$$m_{et} = \frac{I_{et}}{3.91}. \tag{1}$$

I_{et} corresponds to the sum of the integrated areas of the methylene and methyl peaks in the ^{13}C spectra. The amount of exchange in percent, $F(\%)$, is calculated by comparing m_{et} to the mean volume of water released, V_p, for the reference samples by drying at 105°C and corrected for density difference between water and ethanol. $F(\%)$ is represented by eq 2:

$$F(\%) = \frac{m_{et} \cdot 100}{\rho_{et} V_p}, \tag{2}$$

where ρ_{et} is the bulk density of ethanol. The assumption that ethanol in pores has the same density as bulk ethanol is certainly valid if the pore size is much larger than the size of the molecules, but it might be erroneous if the pore size is of the same order of magnitude as the molecule itself. According to MIP investigations [10] of well-hydrated samples of cement paste, pores with radii <82 Å, where a deviation from bulk density may exist (if any), contribute only to 18.6% of the total pore volume. Although not being an ignorable contribution, the measured amounts of exchange are, as we shall see later in this section, consistent with earlier results.

$F(\%)$ vs. exchange time calculated for samples S03, S04, S06, and S10 is plotted in Figure 2 and suggests that the exchange time varies with the w/c ratios. Sample S10 (w/c = 1.0) reaches a constant ethanol content after 1 to 2 days and S06 (w/c = 0.60) after 4 to 5 days. Samples S04 (w/c = 0.40) and S03 (w/c = 0.30) reaches a constant value of ethanol only after 20 to 50 days. The filling factor, $F(\%)$, on the other hand, is about 90% in both S10 and S06 and about 60% in both S04 and S03,

Advn Cem Bas Mat
1998;8:108–117

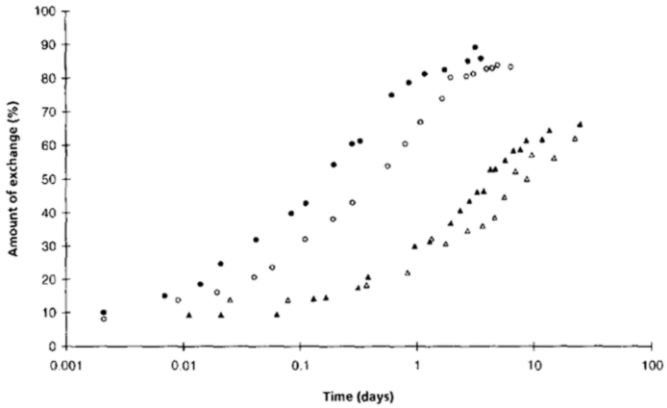

FIGURE 2. The amount of exchange of ethanol with water vs. time during diffusion of ethanol into hydrated cement pastes, S03 (△), S04 (▲), S06 (○), and S10 (●). The amount of exchange or filling factor, $F(\%)$, is given in percent of the expected value calculated from the total amount of water released during preheating at 105°C.

thus dividing the samples in two groups. A filling factor of 60% for w/c = 0.40 is in agreement with earlier measurements [3]. The difference in filling factors can be rationalized in light of the difference in pore size characteristics of the two groups. HCPs with w/c ratios less than about 0.40 have a pore system dominated by micro- and mesopores that are intrinsic to the hydrated cement gel. At higher w/c ratios, coarser capillary pores occur, due to excess water that does not take part in the hydration process. The results from liquid exchange indicate that ethanol easily enters the macropores, but has only partial accessibility to the micropore structure and finer part of the mesopore structure. The reason for this, we believe, is connected to the size of the ethanol molecule, which is then the factor determining the maximum degree of filling of the pore system. As the filling factor is observed to be the same in S03 and S04, it may be argued that the pore systems in these samples can be described by the same relative distribution of micro- and mesopores. This conclusion seems to contradict the arguments presented by Mikhail et al. [11] using Brunauer, Emmzt, Teller (BET) measurements that the smaller pores (with diameters up to 80 Å) increase in width with increasing w/c ratio. A possible explanation for this discrepancy is that ethanol is larger and has potentially different surface chemistry towards the pore walls compared to N_2 (which was used in the BET measurements). Work to clarify these subtle but significant differences is in progress in our laboratory by using probe molecules of different sizes. Another point of concern is the necessity of predrying the specimens when using the BET technique, which might affect the pore size distribution.

A question of concern is whether water is still present in the remaining pores not occupied by ethanol. This question cannot be resolved by ^{13}C-NMR alone, but necessitates use of ^{1}H-NMR.

The higher exchange rate observed in sample S04 compared to S03 might be explained by a larger relative pore volume in S04, which will improve the transport capacity compared to S03. Similar arguments may be applied to S10 and S06.

Exchange Rates

To calculate the diffusion coefficients it is necessary to establish whether the diffusion process is Fickian or not. It has earlier been reported that diffusion into virgin and preheated HCPs of w/c ratio 0.40 could be fitted to Fick's second law [5]. In the following, a model is used to describe the diffusion process of ethanol into the sample in order to calculate the diffusion coefficients within the two samples. Ritger et al. [12] introduced a simple exponential relation:

$$\frac{I_t}{I_0} = k \cdot t^n \tag{3}$$

to describe the general solute release behavior of controlled-release polymer devices, where I_t/I_0 is the fractional solute release, t is the release time, k is a constant, and n is the diffusional exponent characteristic of the release mechanism. Here, we apply eq 3 in an analogous way to describe the fractional amount of solute diffusing into a porous material. I_t/I_0 then describes the fractional amount of ethanol exchanged with water at time t. Ritger et al. [12] have shown that in cases of pure Fickian diffusion, the exponent n has a limiting value of 0.46 for diffusion into a cylinder of infinite length. Depending on the ratio of length to diameter of the sample, Fickian diffusion mechanism is described by $0.43 < n < 0.50$. The dotted curves displayed in Figure 3 are calculated by fitting eq 3 to the observed ^{13}C-NMR peak area data from samples S03, S04, S06, and S10 by a nonlinear least squares technique for $I_t/I_0 < 0.6$. The values determined for the exponent n was found to increase with increasing w/c ratio, i.e., n = 0.442 (±0.060), 0.462 (±0.072), 0.647 (±0.147), and 0.620 (±0.240) for samples S03, S04, S06, and S10, respectively, where numbers in brackets represent 90% confidence intervals. The results suggest that the diffusion can be approximated by Fickian diffusion, which is in agreement with the results obtained by Feldman [13] from gravimetric measurements on replacement of water by propan-2-ol and methanol in hydrated cement pastes. Feldman found a linear behavior between the amount of water being replaced vs. the square root of reaction time:

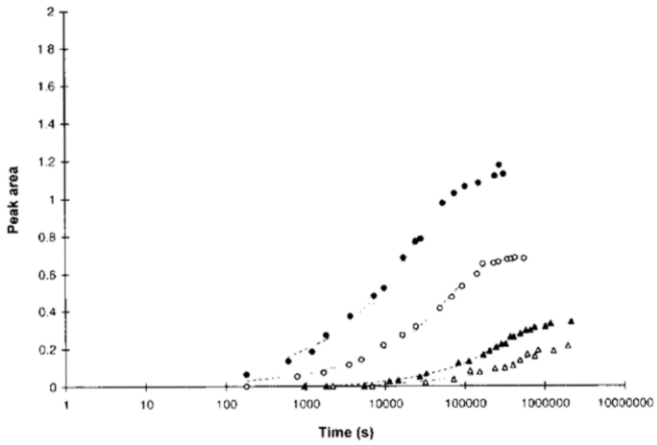

FIGURE 3. Average ^{13}C peak area of methylene and methyl groups in ethanol vs. time during diffusion of the ethanol into hydrated cement pastes, S03 (△), S04 (▲), S06 (○), and S10 (○). The dotted and solid lines are calculated by fitting eqs 3 and 6, respectively, to the experimental data by a nonlinear least squares technique. See text for further details.

$$\frac{W_t}{W_\infty} = 1.127\ \sqrt{\frac{Dt}{L^2}},$$

where W_t and W_∞ are the amounts of alcohol in the sample at time t and at infinite time, respectively. D is the diffusivity and $2L$ is the thickness of the sample.

From these considerations we conclude that the diffusion can be expressed by Fick's second law, which in cylindrical coordinates can be written [12]:

$$\frac{\partial C}{\partial t} = D\left(\frac{\partial^2 C}{\partial r^2} + \frac{1}{r}\frac{\partial C}{\partial r}\right), \tag{4a}$$

where D is the diffusion coefficient and r is the distance from the center of the cylindrical sample. C is the concentration of ethanol at time t at a distance r from the center of the cylinder. In order to find a unique solution of eq 4a, boundary conditions and initial conditions have to be specified. Since the cylindrical cement sample (a cylinder of approximate diameter and height of 5.5 mm and 20 mm, respectively) is confined in an infinite reservoir of ethanol, the boundary condition can be written as:

$$C(r = a,\ t) = C_0, \tag{4b}$$

where C_0 is the (constant) concentration of ethanol at the cement/ethanol surface at any time t. The initial condition satisfies the equation:

$$C(r,\ t = 0) = 0, \tag{4c}$$

since the sample is initially saturated with water and thus contains no ethanol.

TABLE 2. Determination of I_∞ and D in eq 6 by a nonlinear least squares fit to the data presented in Figure 2

Sample	I_∞	D(cm²/s) 10^{-8}	Correl. Coeff. (r^2)
S10	1.108 ± 0.015	59.0 ± 4.6	0.9927
S06	0.676 ± 0.007	23.4 ± 1.4	0.9960
S04	0.336 ± 0.004	4.92 ± 0.22	0.9967
S03	0.217 ± 0.013	2.65 ± 0.46	0.9751
S1	0.991 ± 0.026	12.8 ± 0.14	0.9881
S2	0.998 ± 0.023	43.8 ± 0.57	0.9978

Note: Samples S1 and S2 are taken from reference 5 and included for comparison.

The Laplace transform of eq 4a under the specified conditions described by eqs 4b and 4c gives [14]:

$$r^2\frac{\partial^2 \hat{C}}{\partial r^2} + r\frac{\partial \hat{C}}{\partial r} - r^2\frac{p}{D}\hat{C} = 0, \tag{5}$$

where $\hat{C}$ is the Laplace transform of C. Equation 5 represents the Bessel differential equation and can be solved analytically. By taking the inverse Laplace transform of $\hat{C}$, the concentration $C(r, t)$ at any time t and any position r can be determined. The total concentration of ethanol in the sample at time t must be determined by integrating [15] $C(r, t)$ with respect to r from $r = 0$ to $r = a$:

$$\frac{I_t}{I_\infty} = \left(1 - 4\sum_{n=1}^{\infty}\frac{1}{\alpha_n^2}\mathrm{Exp}\left(-\alpha_n^2 D\frac{t}{a^2}\right)\right), \tag{6}$$

where I_∞ is the intensity at equilibrium (infinite time). The terms α_n are the positive roots of $J_0(a\alpha_n) = 0$, where J_0 is the zero-order Bessel function of the first kind. Equation 6 converges slowly, so it has been necessary to use eight terms in the model fit. The α_n values are $\alpha_1 = 2.405$, $\alpha_2 = 5.520$, $\alpha_3 = 8.654$, $\alpha_4 = 11.79$, $\alpha_5 = 14.93$, $\alpha_6 = 18.07$, $\alpha_7 = 21.21$, and $\alpha_8 = 24.35$. Thus, two adjustable parameters, D and I_∞ (which is a relative factor connected to the amount of pore liquid in the different samples), are involved in the curve fitting. The results of this nonlinear least squares fit are summarized in Table 2 and represented by the solid curves in Figure 3. The diffusion coefficients determined for the four samples S03, S04, S06, and S10 are, within a 95% confidence interval, significantly different. An interesting observation is that the diffusion of ethanol in sample S2 (preheated) is almost three times faster than S1 (virgin). This is in agreement with earlier work [16,17] suggesting that drying reduces the internal microsurface area of the HCP, implying an opening of the pore system on preheating.

The measured exchange rate in sample S1 is two to

Advn Cem Bas Mat
1998;8:108–117

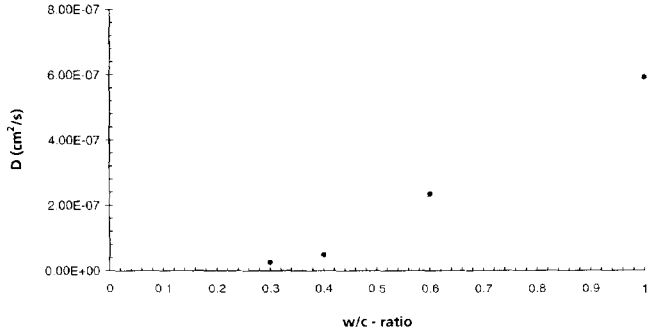

FIGURE 4. Calculated diffusion coefficients vs. w/c ratio for samples S03, S04, S06, and S10. Dotted lines mark 90% confidence interval. The diffusion coefficient determined at w/c ratio 0.30 falls outside this interval.

three times higher than in sample S04, although the w/c ratio is the same. This is rationalized as samples S1 and S2 were only 3 months old against 3 years for samples S10 to S03. The observed difference fits well with the observation that the pore structure in cement paste becomes finer and denser as the hydration process progresses.

Practical Consequences

A knowledge of the time required to reach sufficient exchange is important when working with liquid replacement techniques. The rather long exchange times observed for samples S04 and S03 are of less interest in microscopy where sufficient ethanol exchange is critical only in a sample thickness of about 100 μm. However, people working with larger samples, for example, in MIP, should bear in mind that samples with very fine pore structure may require several weeks of immersion in ethanol for sufficient exchange to take place. The fraction of exchange of ethanol with water at certain time t will depend on the sample radius, a, according to eq 6 and implies that an increase of the cylinder radius from a = 2.75 mm to a = 5 mm will increase the exchange time in a sample with a pore structure as in S03 from 19.5 to 65 days.

Diffusion Coefficients vs. w/c Ratio

Figure 4 shows a plot of the diffusion coefficients vs. w/c ratio and shows a linear behavior from w/c = 0.4 to w/c = 1.0. The diffusion coefficient at w/c = 0.30 falls outside a 90% confidence interval and is rationalized according to the previous observation that the pore system of HCPs at w/c ratios below about 0.40 is dominated by micro- and mesopores, whereas at higher w/c ratios, capillary pores appear resulting from excess water that does not take direct part in the cement hydration process.

^{1}H- and ^{13}C-NMR

The ^{13}C data only give information about the ethanol content. A direct measurement of the ethanol/water ratio requires observation of both ^{1}H- and ^{13}C-NMR intensities. If fast exchange conditions are valid, both ^{1}H and ^{13}C signal intensities (area) are directly proportional to the number of molecules present. The number of moles of any species can thus be determined if the proportionality constants are known. Sample S1 was saturated with H_2O and sample S2 was presaturated with D_2O. The proportionality factors were determined simply by combining the observed proton and carbon intensity vs. "reaction" time.

Equations 7a through 7c are generally valid and make it possible to determine the proportionality factors k^H and k^C relating the proton and carbon NMR intensity to the number of moles of protons and carbons in the system, respectively:

$$n_{H_2O}M_{H_2O} + n_E M_E = m_T, \tag{7a}$$

where n_i represents the number of moles of water (i = H_2O) and ethanol(i = E), respectively. M_i is the corresponding molecular weight of species and m_T is the total amount of ethanol and water in the sample. The total carbon and proton NMR intensities, I_T^C and I_T^H, can be expressed by eqs 7b and 7c:

$$2k^H n_{H_2O} + 6k^H n_E = I_T^H \tag{7b}$$

$$k^C n_E = I_T^C. \tag{7c}$$

The factors 2 and 6 in eq 7b originate from the number of protons of the water molecule and the ethanol molecule, respectively.

The D_2O-saturated cement paste, S2, contains no observable water protons and makes it possible to determine the k^H/k^C ratio by combining eqs 7b and 7c, with n_{H_2O} = 0:

$$I_T^H = 6\,\frac{k^H}{k^C}\,I_T^C. \tag{7d}$$

A plot of I_T^H vs. I_T^C is depicted in Figure 5. As already emphasized, the two intensities are measured at the same times during the diffusion process. As noticed from the results presented in Figure 5, eq 7d is valid in the initial part of the "reaction," but deviates from linearity at longer exchange times. This behavior can be rationalized according to the reaction:

$$CH_3CH_2OH + D_2O = CH_3CH_2OD + HOD,$$

where the deuterium atoms of some deuterated water molecules are replaced by hydrogen atoms from the

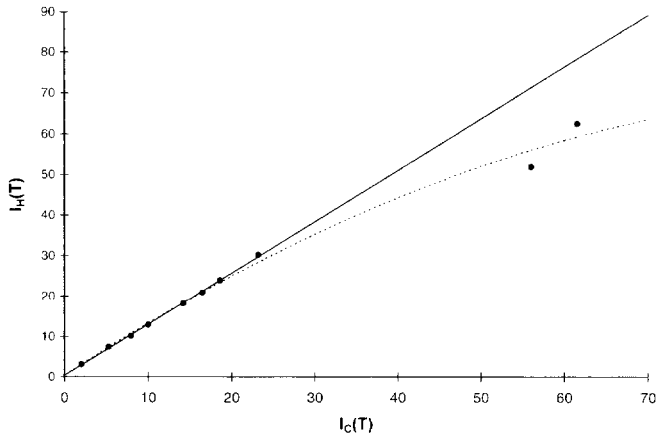

FIGURE 5. Total proton intensity, $I_H(T)$, vs. total carbon intensity, $I_C(T)$, as measured during the diffusion of ethanol into the D_2O-saturated cement paste S2. The straight line is determined by a linear least squares fit using eq 7d.

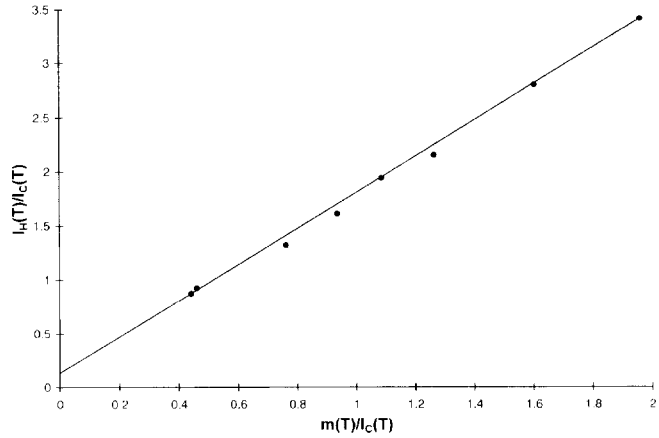

FIGURE 6. The plot shows I_T^H/I_T^C vs. m_T/I_T^C. From the linear least squares fit, it is possible to determine k^H.

hydroxyl group in the ethanol molecule. Thus, some of the protons disappear as HOD, which diffuses out of the solution, and renders the proton intensity less than what is predicted by eq 7b. Only the intensities observed during the first 3 hours are therefore used to calculate k^H/k^C in eq 7d. A linear least squares fit to the observed data (covering the first 3 hours) is represented by the solid line in Figure 5. The slope is 1.264 ± 0.051 and the intercept with the Y-axis, 0.42 ± 0.72. 90% confidence intervals are used to specify uncertainties.

In the case of ethanol diffusing into a water-saturated cement paste (S1), all three equations (7a through 7c) must be combined, giving:

$$\frac{I_T^H}{I_T^C} = \frac{2k^H}{M_{H_2O}} \cdot \frac{m_T}{I_T^C} + \left(6 - 2\frac{M_E}{M_{H_2O}}\right)\frac{k^H}{k^C}. \qquad (7e)$$

Figure 6 shows I_T^H/I_T^C vs. m_T/I_T^C, and makes it possible to determine k^H by a linear least squares fit. $2k^H/M_{H_2O}$ represents the slope and $(6 - 2\,M_E/M_{H_2O})\,k^H/k^C$ the intercept. The value of k^H/k^C, as previously determined, was substituted in the second term of eq 7e before curve fitting. The results are summarized in Table 3.

The dataset from the deuterated sample S2 was used to calculate k^H and k^C. Using the ^1H dataset from sample S1 resulted in a considerably larger uncertainty in the determination of k^C (k^C = 97.3 ± 42.3 area/mg).

Then, entering the equilibrium value of I_T^H and I_T^H for S2 and using k^C = 69.80, gives m_T = 23.0 mg, which is 8% lower than the gravimetrically determined value of 24.9 mg. This difference of 8% is acceptable within the experimental uncertainty in NMR intensity, which is between 5% and 10%. It may thus be concluded that the remaining pore volume (not containing ethanol) is occupied by water, which is approximately 40% (volume by volume) at w/c = 0.30 and 0.40 and approximately 10% at w/c = 0.60 and 1.0. These values are well below the water content [7] where damage can occur to the pore structure through drying due to internal forces created by the water liquid meniscus. It thus shows that sufficient exchange (using ethanol) to avoid damage may be achieved in the w/c ratio range from 0.30 to 1.0.

In the next section an estimate of the mole fraction of ethanol, X_E, from deconvolution of the ^1H-NMR spectra will be discussed.

Deconvolution of ^1H-NMR Spectra

In this section, preliminary work to correlate ^1H-NMR chemical shifts to the mole fraction of ethanol is presented. The proton spectra sampled during the exchange of ethanol with water showed mainly a broad peak with no observable fine structure (Figure 7). In addition to proton-proton dipolar interaction, the broadening of the lines is caused by a combination of: (1) field inhomogeneity, originating from magnetic susceptibility differences between the cement matrix and the confined liquid; (2) exchange of protons between water molecules and hydroxyl protons of ethanol; and (3) a reduction in molecular mobility due to pore wall restrictions. As mentioned earlier, the proton NMR spectrum is expected to be composed of only three

TABLE 3. Determination of calibration factors k^H and k^C from observed proton and carbon intensities vs. diffusion of ethanol into water saturated cement pastes (see eq 7e)

Calibration Factor	Value
k^H/k^C	0.2151 ± 0.0015
k^H	15.01 ± 0.42
k^C	69.80 ± 0.50

Advn Cem Bas Mat
1998;8:108–117

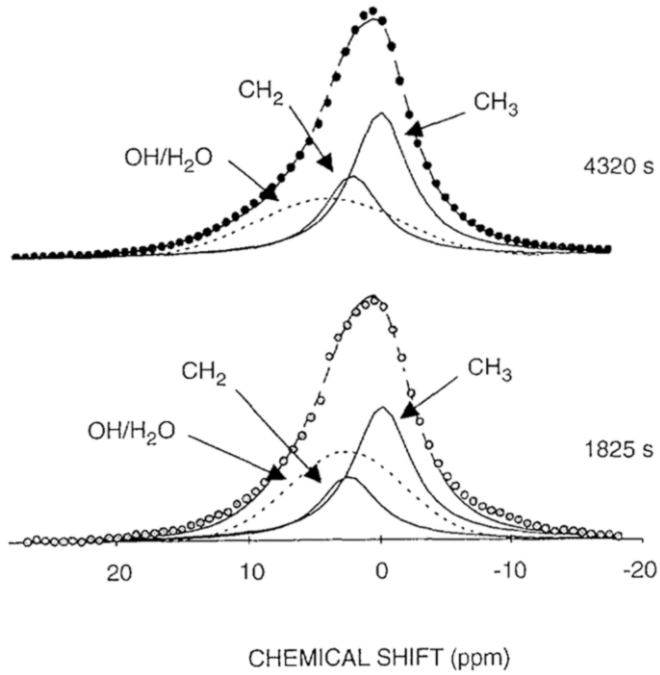

FIGURE 7. ^{1}H-NMR spectra at two different times during the diffusion process, showing the peak shapes of the different resonances, as determined by a nonlinear least squares technique. See text for further details.

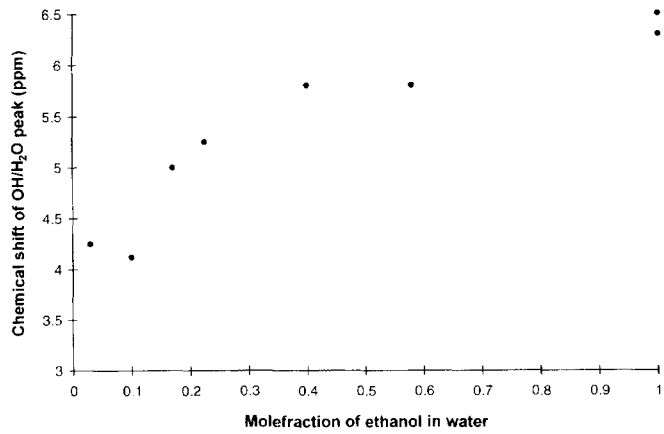

FIGURE 8. Chemical shift of the OH/H_2O resonance vs. mole fraction of ethanol/water mixtures within a cement paste (S1), as determined during the exchange of water with ethanol.

lines, corresponding to methyl, methylene, and OH/H_2O protons, respectively. There are two common line shape functions found in spectroscopy, the Lorentzian line shape and the Gaussian line shape [18]. We have no reasonable arguments to believe that the line shape of the methyl and methylene peaks deviate significantly from the purely Lorentzian line shape functions observed in bulk liquids. The OH/H_2O resonance peak, however, involves an exchange of OH protons and water protons and might therefore not be adequately described by a purely Lorentzian line shape function. Moreover, since the distribution of ethanol and water varies both in time and space, we believe—to a first approximation—that the overall line shape of these protons can be better described by a Gaussian function rather than a Lorentzian function. A preliminary fit of the observed spectra using a sum of two Lorenzian and one Gaussian line shape functions suggested that the chemical shift difference between the methyl and the methylene protons to be constant and equal to 2.42 ppm. Also, the linewidth (at half height) of these peaks were found—within experimental error—to be constant and equal to 5.44 ± 0.50 ppm.

Based on these preliminary findings and the constraint that the intensity ratio between the CH_3 and the CH_2 peaks must be 3:2, all the spectra were refitted under the previously mentioned constraints/conditions. This procedure enabled us to stabilize the computations considerably and showed that the linewidth of the OH/H_2O peak was nearly constant (7.7 ppm), and that the chemical shift increased with increasing ethanol concentration (Figure 8), which is also observed in water/ethanol bulk mixtures in our laboratory. This empirically derived correlation between the chemical shift and ethanol concentration (Figure 8) makes it possible to estimate the concentration of ethanol in the pore system of the cement paste by simply performing a curve fit of the observed ^{1}H-NMR spectrum under the conditions outlined previously.

A more detailed and comprehensive analysis of the OH/H_2O peak line shape is in progress using methanol instead of ethanol.

Conclusions

A linear relationship between ^{13}C-NMR peak intensities and gravimetrically determined amount of ethanol inside the pore system of HCPs is observed for w/c ratio from 0.30 to 1.0. Although cement pastes made with different w/c ratios exhibit different relative amounts of micropores and capillary pores resulting in a varying average environment experienced by the pore fluid, no observable effects on ^{13}C-NMR peak intensities resulting from such variations were present in the w/c ratio range used. Quantitative ^{13}C-NMR may therefore be applied successfully for ethanol within the pore structure of HCPs.

The diffusion of ethanol was shown to be described by Fickian diffusion, assuming one-dimensional diffusion under perfect sink boundary conditions.

The diffusion coefficients determined for the four samples S03, S04, S06, and S10 are significantly different and vary between 2.65×10^{-8} for w/c = 0.30 and 5.9×10^{-7} for w/c = 1.0.

For the 5.5 × 10 mm cylindrical samples, the time needed to reach 90% (t_{90}) and 95% (t_{95}) of maximum possible exchange is between 1 to 2 days for the sample with the higher w/c ratios and 2 to 3 weeks for the two denser samples. This difference should be kept in mind when working with larger samples, for example, in MIP. Due to the $\exp(-Dt/r^2)$ correlation between the fraction of exchange, exchange time, and sample radius, an increase of sample radius to 5 mm will increase the exchange time in a sample with pore structure like S03 from 19.5 to 65 days.

The maximum achievable filling factor, $F(\%)$, separates the samples into two groups. $F(\%)$ is calculated to approximately 60% for samples dominated by micro- and mesopores (w/c = 0.30 and 0.40) and 90% for samples that additionally contain capillary pores (w/c = 0.60 and 1.0). The pore size distribution at the two w/c ratios 0.30 and 0.40 seems to be similar when considering the ratio between the volume occupied by ethanol and the remaining volume still occupied by water.

There is a linear relationship between D and w/c ratio in the w/c ratio range from 0.40 to 1.0. w/c ratio 0.30 falls outside the 90% confidence interval.

The mole fraction of ethanol was determined from the observed carbon and proton intensity vs. reaction time by comparing H_2O-saturated and D_2O-saturated samples. Water was found to occupy the remaining volume not accessible to ethanol. In the tested w/c ratio range and at the end of the exchange process, the water content is below the values where damage to the pore structure normally occurs due to internal tension.

An empirical relation between chemical shift of the OH/H_2O peak and mole fraction of ethanol is found and makes it possible to estimate the mole fraction from a simple spectral analysis.

References

1. Feldman, R.F.; Beaudoin, J.J. *Cem. Concr. Res.* **1991,** *21,* 297–308.
2. Bager, D.H.; Sellevold, E.J. *Cem. Concr. Res.* **1979,** *9,* 653–654.
3. Gran, H.C. *Cem. Concr. Res.* **1994,** *25,* 1063–1074.
4. Sandström, M. Swedish National Testing Institute, Report SP-AR **1988**: 43, **1988,** *31;* or NORDTEST-Build No., 677–687.
5. Gran, H.C.; Hansen, E.W. *J. Magn. Reson. Imaging* **1996,** *14,* 903–904.
6. Taylor, H.F.W. *Cement Chemistry;* Academic Press: New York, 1990.
7. Powers, T.C.; Browneyard, T.L. *Res. Labs. Portland Cement Association, Bulletin 22* (March 1948).
8. Sanders, J.K.; Hunter, B.K. *Modern NMR Spectroscopy: A Guide for Chemists;* Oxford University Press: New York, 1988.
9. Bhattacharja, S.; Moukawa, M.; D'Orazio, F.; Jehng, J.; Halperin, W.P. *Adv. Cem. Based Mater.* **1993,** *1,* 67–76.
10. Winslow, D.N.; Diamond, S. *J. Mater.* **1970,** *5,* 564–585.
11. Mikhail, R.S.; Copeland, L.E.; Brunauer, S. *Canad. J. Chem.* **1964,** *42,* 426–437.
12. Ritger, P.L.; et al. *J. Controlled Release* **1987,** *5,* 23–36.
13. Feldman, R.F. *Cem. Concr. Res.* **1987,** *17,* 602–612.
14. Abramowitz, M.; Stegun, I.A. *Handbook of Mathematical Functions.* Dover Publications: New York, 1970.
15. Wilson, A.H. *Phil. Mag.* **1948,** *39,* 48–58.
16. Hunt, C.M.; Tomes, L.A.; Blaine, R.L.J. *Res. Nat. Bur. Std.* **1960,** *2,* 163–169.
17. Powers, T.C.; Copeland, L.E.; Hayes, J.C.; Mann, H.M. *ACI Journal,* **1954,** *November,* 285–298.
18. Shaw, D. *Fourier Transform NMR Spectroscopy;* Elsevier Science: New York, 1976.